

## Numerical investigation of optically induced director oscillations in nematic liquid crystals

G. Demeter\* and L. Kramer

*Physikalisches Institut der Universität Bayreuth, D-95440 Bayreuth, Germany*

(Received 24 April 2001; published 24 July 2001)

We present a theoretical study of the effects induced by the passage of a linearly polarized light beam through a thin cell of homeotropic nematic liquid crystal. The light is incident at a slightly oblique angle and is polarized perpendicular to the plane of incidence. Experiments in this geometry have revealed a rich variety of complex, time dependent director motion. We solve numerically the director equations for the nematic and compare the results with existing experimental findings.

DOI: 10.1103/PhysRevE.64.020701

PACS number(s): 61.30.-v, 42.70.Df, 05.45.Pq, 42.65.Sf

Liquid crystals (LCs) are very interesting anisotropic optical materials that have been investigated thoroughly for decades. In particular, phenomena associated with the so-called light-induced director reorientation in nematics have been intensively investigated both theoretically and experimentally [1]. These phenomena occur when the intensity of the light incident on the LC is sufficiently large so that the orienting effect of the electric field of the light overcomes the elastic forces opposing reorientation in the nematic. The simplest of all these phenomena is the ordinary light-induced Fréedericksz transition (LIFT) in various geometries.

One particular geometry of light-induced director reorientation that has aroused considerable interest is the case of a linearly polarized plane wave incident on a thin cell of homeotropically aligned nematic LC at a small angle  $\alpha$  (Fig. 1). The direction of polarization is perpendicular to the plane of incidence (ordinary wave). Experiments revealed that as the intensity of the light is increased the director starts oscillating. These oscillations are at first periodic and regular, but at higher intensities various dynamical regimes and even a transition to chaos can be observed [2,3]. Chaotic oscillations have been reported in only one other geometry and only very recently [4]. A theoretical model involving a few discrete reorientation modes showed that in the geometry mentioned above one can indeed expect chaotic dynamics in the system, and can even hope to observe a peculiar route to chaos through a cascade of gluing bifurcations [5]. Recent experiments [6–8] seem to verify some predictions of the model, but not all. In particular, there is clear experimental evidence for the occurrence of the first gluing bifurcation [8], but no clear evidence for any further bifurcations of the cascade. Furthermore, the onset of chaos is observed to be at much higher intensity than that predicted by theory.

In an attempt to shed light on the cause of this discrepancy between the model [5] and experiments [7,8], we have performed numerical simulations of the basic equations that describe the system. We consider the setup depicted in Fig. 1 with strong anchoring of the nematic at the boundaries of the cell. The equation that describes the evolution of the director

$\mathbf{n}(\mathbf{r}, t)$  can be deduced from the free energy of the nematic that contains two contributions: the elastic energy of the nematic and its dielectric energy in the light wave [1]. By this we assume that backflow effects can be absorbed into the renormalization of the orientational viscosity constant  $\gamma$  and consider only the director to be an active dynamical variable. We also assume the director to depend only on the  $z$  coordinate and for further simplicity apply the one-constant approximation to the elastic free energy, i.e.,  $K_1 = K_2 = K_3 = K$ . The equations for the director components thus become

$$\gamma n_k = K \partial_z^2 n_k + \frac{\epsilon_a}{8\pi} E_k n_i E_i - \lambda n_k, \quad (1)$$

where  $K$  is the elastic coefficient and  $\epsilon_a = \epsilon_{\parallel} - \epsilon_{\perp}$  the dielectric anisotropy in the optical regime. (Indices appearing twice in a product imply summation over that index.)  $\lambda$  is a Lagrange multiplier that maintains  $n_i n_i = 1$  during the course of time and is

$$\lambda = n_i K \partial_z^2 n_i + \frac{\epsilon_a}{8\pi} (n_i E_i)^2. \quad (2)$$

These equations must be augmented by the self consistency relation that  $\mathbf{E}(z, t)$  is a solution of Maxwell's equation. We assume the nematic to be a transparent dielectric with a position-dependent dielectric tensor  $\epsilon_{ij} = \epsilon_{\perp} \delta_{ij} + \epsilon_a n_i n_j$ . The parameters the equations contain are the material parameters  $K$ ,  $\gamma$ ,  $\epsilon_{\perp}$ ,  $\epsilon_a$ , the wavelength of the light  $\lambda_L$ , the thickness of the cell  $L$ , the angle of incidence  $\alpha$  and the

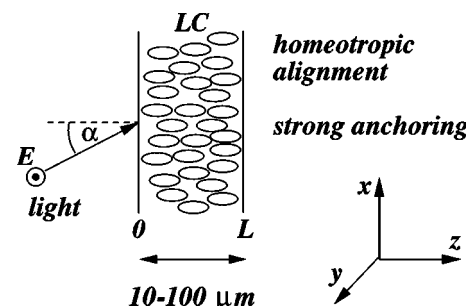


FIG. 1. Geometry of the setup: an ordinary wave incident on a cell of homeotropic nematic at a slightly oblique angle.

\*On leave from the Research Institute for Particle and Nuclear Physics of the Hungarian Academy of Sciences, Budapest, Hungary.

intensity of the light  $I$ . From theory [5] it is clear however, that the number of parameters that are essential to describing qualitative behavior in the system is considerably less than eight. First,  $\gamma$  appears only in the constant  $\tau_d = \gamma L^2 / \pi^2 K$  that merely sets the timescale for the phenomena. Apart from  $\tau_d$ ,  $K$  appears only together with the light intensity—and can be included in a dimensionless intensity parameter  $\rho = I/I_F$  where  $I_F = [\pi^2 c(\varepsilon_\perp + \varepsilon_a)K/L^2 \varepsilon_a \sqrt{\varepsilon_\perp}]$  is the threshold intensity for the LIFT. The dependence on  $L$ ,  $\lambda_L$ ,  $\varepsilon_\perp$  and  $\varepsilon_a$  can be simplified by introducing the parameter  $\kappa = [L \sin^2(\alpha) \varepsilon_a / \lambda_L \sqrt{\varepsilon_\perp} (\varepsilon_\perp + \varepsilon_a)]$ . The equations now depend only on  $\rho$ ,  $\kappa$ ,  $\beta = \varepsilon_a / \varepsilon_\perp$  and  $\alpha$ . Furthermore, the explicit dependence on  $\alpha$  is only through terms such as  $1 + \sin^2(\alpha)$ , which is very weak for the angles in question ( $\alpha \leq 12^\circ$ ). So we are left with three essential parameters:  $\rho$ ,  $\kappa$  which can be thought of as the angle parameter, and the material parameter  $\beta$ . This latter varies little between different materials in the optical regime.

Equations (1) and (2) together with Maxwell's equation were the starting point of our investigations. To solve this set of nonlinear partial differential equations we have used an implicit Crank-Nicholson finite-difference scheme which proved to be stable and fast. To calculate the electric fields we solved Maxwell's equations with an adaptive Runge-Kutta algorithm. The data which the simulation produced were the values of the three director components at a series of points in space at each timestep. To reduce the amount of data and to obtain quantities that give better insight into the evolution of the director, we first singled out the  $x$  and  $y$  components of the director. The assumption of strong anchoring allows us to expand these components as  $n_x(z,t) = \sum_m A_m(t) \sin(m\pi z/L)$ ,  $n_y(z,t) = \sum_m B_m(t) \sin(m\pi z/L)$ . Since the higher order modes are strongly damped by elasticity (see Refs. [5,1]), only the amplitudes of the first few modes are of non-negligible magnitude so the system effectively reduces to a finite-dimensional one.

The present simulation improves over the theoretical model of Ref. [5] in several aspects. First, the reorientation and hence, the mode amplitudes were assumed to be small in the model and a perturbation expansion was employed that was correct to third order. Second, the smallness of the angle of incidence was explicitly used in the model to simplify formulas. These assumptions were discarded in the present simulation. Note that the assumption that we need to include only the first few sine modes for the director components was used in the simulation only to reduce the amount of data to store. It was not used during the calculation and its validity was explicitly checked when determining the number of modes to save. The assumption that we are dealing with a plane wave and that the director depends only on the  $z$  coordinate was kept, however, and so was the assumption that flow does not play a major role in the dynamics. When solving Maxwell's equations, we also kept the assumption that the director changes very slowly on the spatial scale of the wavelength of light, thus reflection within the material is negligible. One simplification that was not used in the model but was applied in the simulation was the one-constant approximation for the elastic energy. We argue, however, that this should not cause a great difference in the results, as

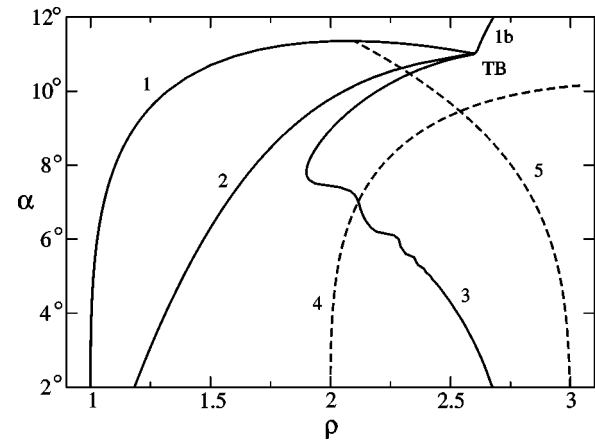


FIG. 2. Bifurcation diagram as a function of the dimensionless intensity of light ( $\rho$ ) and the angle of incidence ( $\alpha$ ). The lines are explained in the text.

setting  $K_1 = K_2 = K_3$  in the model results only in slight numerical differences in the parameter values at which bifurcations occur, the overall behavior is not affected. This is to be expected as the dominant nonlinear terms in the model are those containing the electric field of the light, while the ones containing the difference of the elastic constants contribute very little.

The behavior of the system was investigated with the help of the simulations as a function of  $\rho$  and  $\alpha$ . For the material parameters we used values that correspond to the chemical E7 that was used in the experiments [9–11] and we took  $L = 50 \mu\text{m}$ . Our results can easily be carried over to any cell thickness, however, by noting that the essential parameter is  $\kappa \sim L \sin^2(\alpha)$ . Figure 2 shows the curves for the first three bifurcations on the  $\rho$ - $\alpha$  plane. Curve 1-1b is the line of primary instability, where the state of homogeneous homeotropic orientation (the basic state) becomes unstable. It consists of two sections, which join in a Takens-Bogdanov (TB) point. For small angles the basic state loses stability in a stationary bifurcation (1), for larger angles in a Hopf bifurcation (1b). At the stationary instability two new symmetry degenerate stationary states (fixed points) are created, which are images of each other under the transformation  $S: y \rightarrow -y$ , the symmetry of the setup. As the intensity of the light is increased, these stationary states lose stability in a Hopf bifurcation at line 2, where two symmetry degenerate limit cycles are created [Fig. 3(a)]. Line 3 is the line of the first gluing bifurcation. At this point, the limit cycles born in the secondary Hopf bifurcation are homoclinic orbits to the basic state [Fig. 3(b)] and above it they join to form a single, symmetric, double-length limit cycle [Fig. 3(c)].

This sequence of events agrees with calculations from the model. The most important difference is that the line of the first gluing takes a sudden turn towards high intensities as the angle is decreased, whereas the model predicts that it remains close to the line of the Hopf bifurcation. The model also predicts that in some range of angles around  $7^\circ$  the first gluing bifurcation is followed by a cascade of further gluings that lead to a strange attractor [5,12]. In the simulation however, we could not find this cascade of gluings.

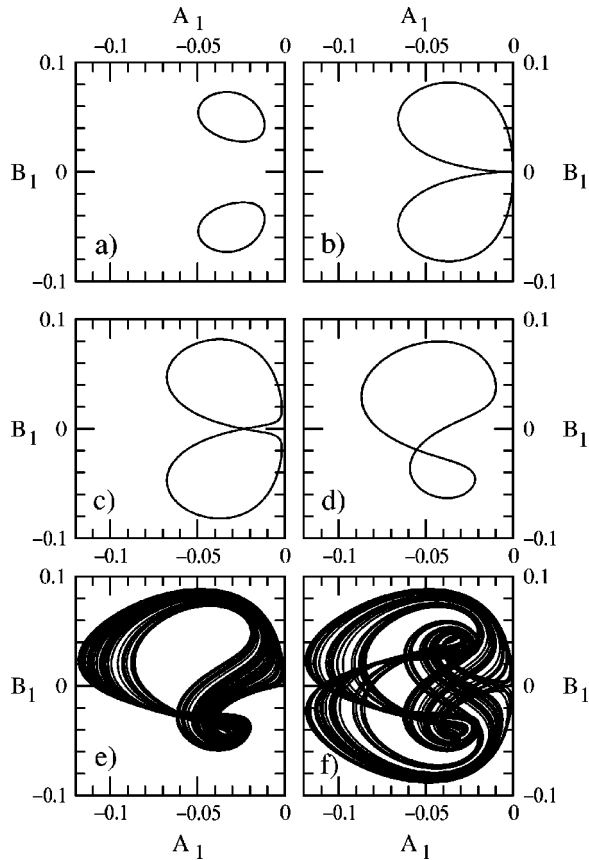


FIG. 3. Projection of limit cycles on the  $A_1$ - $B_1$  plane for  $\alpha = 9.5^\circ$  and (a)  $\rho = 2.0$ , (b)  $\rho = 2.0885$ , (c)  $\rho = 2.11$ , and (d)  $\rho = 2.4$ .  $A_1$  and  $B_1$  are dimensionless mode amplitudes characterizing the director orientation (see text). Strange attractors on the  $A_1$ - $B_1$  plane at (e)  $\rho = 2.554$  and (f)  $\rho = 2.56$ .

Actually there is only a very small region in the  $\rho$ - $\alpha$  plane where this cascade may exist at all. There are two necessary conditions for its existence, both of which concern the linear eigenvalues of the system around the basic state [12,13]. (We have a discrete set of eigenvalues as the system effectively reduces to a finite dimensional one.) The basic state at this point is a saddle, and (i) it is to have one single positive eigenvalue  $\Lambda_1$  which is smaller in magnitude than the second largest eigenvalue  $\Lambda_2$  (i.e.,  $-\Lambda_2 > \Lambda_1$ ) and (ii)  $\Lambda_1$  must belong to the subspace spanned by  $\{B_i\}$  and  $\Lambda_2$  must belong to the subspace spanned by  $\{A_i\}$ . Condition (i) is violated to the right of line 4 and this means that the homoclinic orbits are unstable past this line. Condition (ii) is violated to the right of line 5. Thus, the small region enclosed by lines 3, 4, and 5 is the only one where the gluing scenario may exist at all. We have scanned this region of parameter space to find it, but our search gave a negative result.

Nevertheless our simulations do predict complex nonlinear and chaotic behavior of the system in various parameter ranges. As an illustration, we consider the sequence of events after the first gluing bifurcation at  $\alpha = 9.5^\circ$ . The symmetric limit cycle loses stability in a fourth bifurcation and two symmetry degenerate, asymmetric limit cycles are born. These then undergo a period doubling sequence and two asymmetric strange attractors are created [Figs. 3(d) and

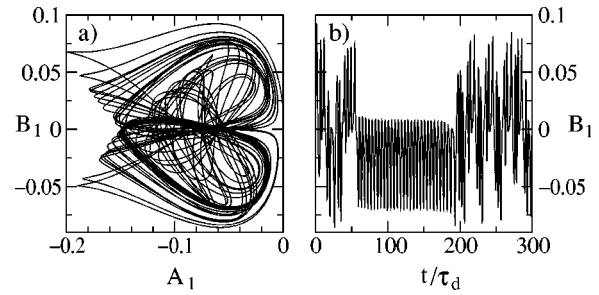


FIG. 4. Intermittent behavior at  $\alpha = 9.5^\circ$  and  $\rho = 3.2302$  (a) motion projected onto the  $A_1$ - $B_1$  plane. (b) The time evolution of  $B_1$ .

3(e); only one of the symmetry degenerate pair is shown]. These attractors pass closer and closer to the origin as the intensity is increased, and eventually collide or “glue” to create one single, symmetric strange attractor [Fig. 3(f)]. At a considerably higher intensity, we can see the strange attractor disappear and give way to simple limit cycle behavior in what appears to be a tangent bifurcation. The system shows intermittent behavior near the transition as the motion is still controlled by the strange attractor, but it sometimes moves on an almost periodic orbit for considerable amounts of time [Figs. 4(a) and 4(b)]. At a slightly higher intensity a stable limit cycle comes into existence in this region of phase space. Once this happens, it is this limit cycle that defines long-term behavior and stochasticity is seen only as an initial transient.

A detailed comparison of the experimental results of Refs. [7,8] and our simulation done with the same parameters ( $L = 75 \mu\text{m}$ ,  $\alpha = 5^\circ$ ) shows that for low intensities simulation and experiment agree qualitatively. Experiment shows that there is a stationary reorientation of the director between  $\rho = 1$  and  $\rho = 1.6$ , and then regular oscillations whose period increases with intensity until about  $\rho = 1.9$ . By comparison, simulation predicts the secondary Hopf bifurcation to occur at  $\rho = 1.48$  and at  $\rho \approx 1.52$ – $1.54$  there are already sizable oscillations. The period of oscillations is predicted to increase as the intensity increases below the gluing, as observed in the experiment. The first stochastic regime observed in the experiment between  $\rho = 1.9$  and  $\rho = 2$  can presumably be identified with the vicinity of the first gluing bifurcation [8]. The simulation predicts this to be at  $\rho = 2.27$ . After this there is again a regular oscillatory regime until  $\rho = 2.6$ . After the second periodic regime, a second stochastic regime was observed in the experiment between  $\rho = 2.6$  and  $\rho = 3.0$ , after which a regime termed “very stochastic” or chaotic was reported. Alas our simulations do not show chaos at any intensity with the above parameters. There is one further bifurcation in the simulation at  $\rho = 3.6$  where the symmetric limit cycle loses stability and two asymmetric ones are created. This event could give rise to a stochastic regime experimentally, as the system can make random jumps between limit cycles due to noise. However, the intensity at which it occurs is much higher than the intensity range at which the second stochastic regime was observed.

The cause of discrepancy between the simulation and experimental observations is not clear. Several factors may contribute. One is the fact that the experiments were done

with Gaussian beams whose spot size on the sample was comparable to the sample width and were thus far from realizing a plane wave of infinite extension assumed in the model and simulation. The other possible cause may be the fact that in our simulations we assumed that flow does not play a major role in the dynamics. However, the inclusion of backflow effects in a renormalized  $\gamma$  is possible only if the reorientation is not too large [14], so the equations we solve by computer lose their validity above a certain intensity when the amplitudes do become large. For small angles this happens relatively early, for angles closer to the Takens-Bogdanov point this happens much later. Should the role of flow be the main cause for discrepancy between theory and experiment, our simulations would agree better with possible new experiments done at larger angles, closer to the Takens-Bogdanov point. Interesting nonlinear behavior is to be found in abundance also in this regime (an example is the scenario found at  $L=50\ \mu\text{m}$  and  $\alpha=9.5^\circ$  mentioned earlier) but its observation would be more difficult as the amplitude of director motion is much smaller. A further complication is the fact that in several intensity regimes complicated limit

cycles may coexist simultaneously, and since the system may jump from one to another due to noise, these regimes may also appear to be stochastic in the experiment. Distinguishing these from the truly chaotic regimes is not a simple task. It seems favorable to use a thin sample for the experiments, as the range of angles where interesting behavior may be observed (which is bounded from above by the Takens-Bogdanov point) is greater when the sample is thinner.

In conclusion, we can say that our simulations seem to confirm the assumption that the first stochastic regime observed in the experiment corresponds to the first gluing bifurcation in the theoretical model of Ref. [5] as suggested in Ref. [8]. However, the precise nature of the chaotic behavior observed experimentally remains unclear. To clarify it, one would have to achieve better correspondence between theory and experiment. One possibility for this would be to check whether observations at larger angles correspond better to the above theory. Another possibility is the inclusion of the finite beam size and/or flow in the theory. In any case, we must conclude that the understanding of these complex phenomena is far from complete.

- 
- [1] N. V. Tabiryan, A. V. Sukhov, and B. Ya. Zel'dovich, *Mol. Cryst. Liq. Cryst.* **136**, 1 (1985); F. Simoni, *Nonlinear Optical Properties of Liquid Crystals* (World Scientific, Singapore, 1997).
- [2] A. S. Zolotko *et al.*, *Liq. Cryst.* **15**, 787 (1993).
- [3] G. Cipparrone *et al.*, *Phys. Rev. E* **47**, 3741 (1993); V. Carbone *et al.*, *ibid.* **54**, 6948 (1996).
- [4] B. Piccirillo, C. Toscano, F. Vetrano, and E. Santamato, *Phys. Rev. Lett.* **86**, 2285 (2001).
- [5] G. Demeter and L. Kramer, *Phys. Rev. Lett.* **83**, 4744 (1999); G. Demeter, *Phys. Rev. E* **61**, 6678 (2000).
- [6] E. Santamato, P. Maddalena, L. Marrucci, and B. Piccirillo, *Liq. Cryst.* **25**, 357 (1998); E. Santamato, G. Abbate, P. Maddalena, L. Marrucci, D. Paparo, and B. Piccirillo, *Mol. Cryst. Liq. Cryst.* **328**, 479 (1999).
- [7] G. Cipparrone, G. Russo, C. Versace, G. Strangi, and V. Carbone, *Opt. Commun.* **173**, 1 (2000).
- [8] G. Russo, V. Carbone, and G. Cipparrone, *Phys. Rev. E* **62**, 5036 (2000); V. Carbone, G. Cipparrone, and G. Russo, *ibid.* **63**, 051701 (2001).
- [9] For the dielectric constants at optical frequency we took  $\epsilon_{\perp}=2.25$  and  $\epsilon_a=0.76$  from Ref. [10], and the ratio  $K_3/\gamma$  was taken to be  $10^{-6}\ \text{cm}^2/\text{s}$  from a direct measurement in the same geometry [11]. This value should already include the backflow effects. The wavelength of the light was taken to be  $\lambda=514.5\ \text{nm}$ .
- [10] N. V. Tabiryan, A. L. Tabiryan-Murazyan, V. Carbone, G. Cipparrone, C. Umeton, and C. Versace, *Opt. Commun.* **154**, 70 (1998).
- [11] G. Cipparrone, D. Duca, C. Versace, C. Umeton, and N. V. Tabiryan, *Mol. Cryst. Liq. Cryst.* **266**, 263 (1995).
- [12] A. Arneodo, P. Coulet, and C. Tresser, *Phys. Lett.* **81A**, 197 (1981); Y. Kuramoto and S. Koga, *ibid.* **92A**, 1 (1982); D. V. Lyubimov and M. A. Zaks, *Physica D* **9**, 52 (1983).
- [13] Paul Glendinning, *Stability, Instability, and Chaos* (Cambridge University Press, Cambridge, England, 1994).
- [14] B. L. Winkler *et al.*, *Phys. Rev. A* **43**, 1940 (1991).